JOURNAL OF SOLID STATE CHEMISTRY 12, 232–237 (1975)

Characterization of Thin Oxide Films for FET Applications*

C. M. OSBURN

IBM Thomas J. Watson Research Center, Yorktown Heights, New York 10598

Received July 3, 1974

Electronic transport in thin silicon dioxide films used for field effect transistor (FET) devices is controlled by the metal–oxide barrier height rather than by bulk defect centers. The presence of charged ions (i.e., sodium) or interface states at the injecting electrode can lower the barrier height and thereby increase the electronic conduction. In addition, the transport of sodium ions is generally believed to be emission-limited from traps located at the metal–oxide interface. When present in large concentrations ($>10^{12}/cm^2$), Na ions can alter the internal space charge field, markedly enhance the current, and even lead to dielectric breakdown. Instabilities in the current at high electric fields ($\sim 10^7$ V/cm) as a result of ionization processes were observed prior to breakdown. The degradation of metal–oxide–semiconductor capacitors as a result of electrothermal stressing can be retarded by the incorporation of hydrogen in the SiO_2.

Introduction

Present day metal oxide semiconductor field effect transistors (MOSFET's) rely on a thin insulating film between the silicon substrate and the controlling gate electrode. This gate dielectric must satisfy several stringent requirements. It must have a very low conductivity to minimize loss; the level of uncompensated charge (either fixed or mobile) must be very low; the dielectric must be capable of withstanding electric fields of the order of 2 MV/cm without breaking down or degrading; and finally, the dielectric must be uniform with respect to thickness, breakdown strength, and charge levels.

Although several insulators are potentially useful for a MOSFET gate dielectric, silicon dioxide (SiO_2) has been the almost universal choice either by itself or as part of a dual layer. At normal operating conditions the dc conduction of a 1000 Å SiO_2 film is below the detectability limit of most picoammeters (*1–3*). Both fixed and mobile charge levels can generally be controlled to less than a few times 10^{10} charges/cm^2 (*4*, *5*). Likewise, the density of charged states at the Si–SiO_2 interface can be kept low ($\approx 10^{11}/cm^2$ eV, Ref. (*6*)). Silicon dioxide has a dielectric strength of about 10^7 V/cm and is chemically and thermally stable during the various other silicon processing steps.

Fabrication, Structure, and Purity

Although SiO_2 films can be grown by a variety of techniques, simple thermal oxidation of the starting Si wafer generally leads to the best films. In order to obtain uniform and defect-free films, elaborate precautions are taken at each processing step. Carefully polished silicon wafers having a low dislocation count are thoroughly cleaned—often with solutions of $NH_4OH:H_2O_2$, $HCl:H_2O_2$, and HF (*7*). Wafers are then loaded onto quartz boats and oxidized typically between 800 and 1200°C in an O_2 or O_2–H_2O atmosphere. High purity gases are used during oxidation since even 25 ppm of water has been shown to markedly influence the oxidation rate (*8*) and to incorporate much hydrogen (*9*). At the end of the oxidation cycle, the films are generally annealed in an inert gas

* Invited paper.

Copyright © 1975 by Academic Press, Inc.
All rights of reproduction in any form reserved.
Printed in Great Britain

(N_2) at the oxidation temperature to reduce the fixed charge level (*4*). The metal electrode capacitor dots are then deposited, and the MOS samples are annealed again to further reduce charge levels.

Silicon dioxide films prepared in this fashion are generally considered to be amorphous; however, high levels of sodium contamination are known to catalyze crystallization (*10*). One study (*11*) ascribed poor dielectric breakdown characteristics to the presence of crystallites; it is not clear, however, whether the degradation is due to the crystallization or to the field enhancement of the sodium ions. X-ray diffraction measurements (*12*) in the purest SiO_2 films available in this laboratory revealed crystallization which was at least partially caused by the application of the metal (Fig. 1). In addition, X-ray measurements have observed cycles (apparently related to the humidity) in which crystallites appear and later disappear. Strangely enough, however, it was not possible to crystallize these films by oxidizing in steam.

The incorporation of water related species in thin films of SiO_2 has been appreciated for some time (*9*, *13–15*); even so, its importance to material properties has probably been underestimated. Internal reflection spectroscopy has shown that films oxidized in 60 ppm H_2O may contain nearly 10^{21} Si–H bonds/cm^3 near the Si–SiO_2 interface (*9*).

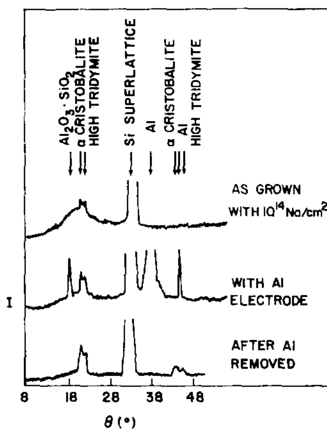

FIG. 1. X-ray diffraction patterns of SiO_2 showing crystallization enhancement by electrode material (Light and co-workers (*12*)).

Water vapor plays a central role in the reduction of interface states. Hydrogen is also important in determining the rate of dielectric degradation under accelerated stress conditions (*17*, *18*) as will be described later. On the negative side, water diffuses rapidly through these films even at room temperature and can create electron trap centers (*6*, *19*, *20*).

Because it is charged, mobile, and abundant, sodium has generally been considered the most important impurity in SiO_2 films used for FET's. Just as hydrogen can be present in different forms, sodium is classified into mobile and immobile species according to whether bias temperature stressing causes a shift of the silicon flatband potential (Fig. 2.) The immobile species is considered to be strongly bound in the glass (perhaps replacing hydrogen in SiOH groups) and not released by electric fields or moderate temperatures (300°C). The mobile species, being less tightly bound, is deleterious to device operation, and extreme care is taken in order to avoid it. The characterization of mobile ions like sodium presents special problems. Many analytical techniques (Auger, ESCA, SIMS, electron microprobe) involve exciting the specimen with charged or highly energetic species; Na is particularly mobile under these conditions and the analyses are in error. Radiotracer techniques and nuclear activation analysis (Fig. 2) have given the best results to date.

When a small amount of a chlorine-containing species is added to the oxidizing

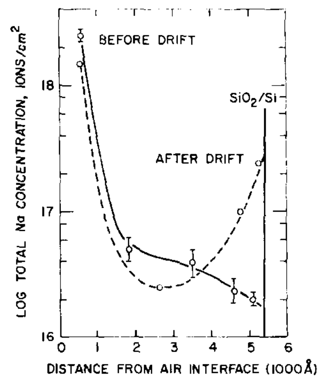

FIG. 2. Sodium profiles in SiO_2 before and after drift at 5×10^5 V/cm and 200°C, showing mobile and immobile components (Yon, et al. (*21*)).

atmosphere (*5*, *17*, *18*, *22–28*), volatile metal chlorides are formed and transported out of the hot region of the furnace tube. This procedure removes heavy metal impurities from the silicon (*28*), increases the minority carrier lifetime (*22*, *23*, *27*, *28*), and gives oxides that have low mobile charge (*5*, *24–26*). When oxidation is done at very high temperatures (1100°C) and concentrations, the chlorine introduces a center which will actually trap and neutralize sodium ions (*5*, *24–26*, *29*). Several studies (*25*, *26*, *29–31*) have focused on the incorporation of Cl in SiO_2. Nuclear backscattering has been the most successful technique for analyzing Cl profiles. The profile itself depends on the additive species and increases with increasing concentration, and oxidation temperature. Oxides grown in HCl have a narrow Cl peak that is located near the Si–SiO_2 interface; the peak is considerably wider and higher for Cl_2 oxides as seen in Fig. 3. The Cl follows the oxidizing interface (Si–SiO_2) during subsequent oxidation in O_2 but is mostly removed during later oxidation in water vapor.

Electrical Conduction

In contrast to bulk materials, many thin films including SiO_2 do not exhibit ohmic conduction at moderately high electric fields. Because of its wide gap and low defect density, the number of free carriers is small compared to the number that can be excited by the applied field. In SiO_2 it is believed that carriers are injected at the contact barrier and are rapidly swept through the film according to a Fowler–Nordheim model (*1–3*). Electrons from the metal (or Si) conduction band tunnel through the triangular barrier formed by the oxide conduction band. The current density, J, through the oxide varies with the applied field, E, as

$$J \propto E^2 \exp\{-K\phi^{3/2}(m^*)^{1/2}/E\},$$

where ϕ is the injecting barrier height, m^* is the relative electron effective mass in the SiO_2 and K is a constant. Conduction data for several injecting metals are given in Fig. 4. Analysis of the slope of the J/E^2 vs $1/E$ plots gives the value of $\phi^{3/2}(m^*)^{1/2}$; by assuming $m^* = 0.5$, very good agreement is reached with barrier heights measured by photoemission.

Since it provides a measure of the contact barrier height, conduction measurements are useful as another tool to characterize the metal–SiO_2 interface. Just as cesium lowers the work function of metals, sodium ions can lower the Si–SiO_2 barrier. When controlled amounts of sodium are intentionally diffused

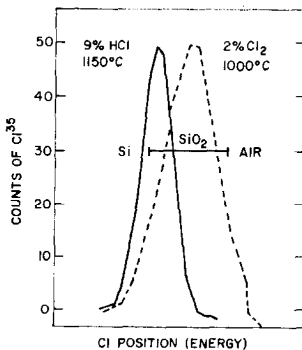

FIG. 3. Comparison of the incorporated Cl profile for HCl and Cl_2 oxides (van der Meulen and others (*29*)).

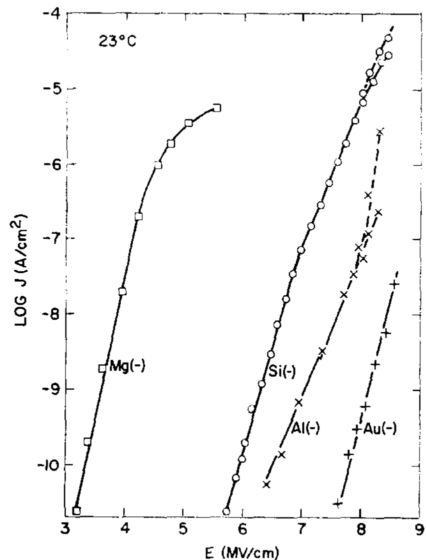

FIG. 4. Electrical conduction in SiO_2 showing the influence of the injecting metal (Osburn and Weitzman (*3*)). The solid line represents the instantaneous value and, the dashed line represents the steady state value at high fields.

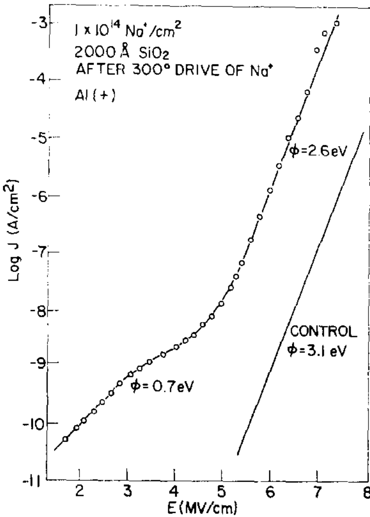

FIG. 5. Electrical conduction in a Na contaminated SiO_2 from showing regions of high and low injecting barrier heights (Osburn and Ormond (*32*)).

through SiO_2 to the Si interface, the electrical conduction changes systematically with Na level in a way to reflect a lowered barrier (*32*). Even more interesting are the results of DiStefano (*33*, *34*) as well as Williams and Woods (*35*), which show that the effect of Na is often localized; electrical conductivity measurements also reflect this localization (see Fig. 5) since the low field barrier height can be considerably lower than the high field one.

Ionic (Sodium) Motion

Two techniques have been extensively used to electrically characterize ionic motion in SiO_2 (*36–39*): (1) measurement of the shift in the silicon flatband potential using capacitance–voltage (*C–V*) curves and (2) measurement of the polarization charge as a function of time (*Q–t*). Assuming the charge is located at the metal–oxide interface at time $t = 0$, shifts in the flatband potential, V_{FB}, or in the polarization charge, Q, can be related to the moment of the charge, e, in the oxide

$$\Delta V_{FB}(t) = (-l)\cdot \Delta Q(t) = -\frac{1}{\varepsilon}\int_0^l x\rho(x,t)\,dx = -\frac{1}{\varepsilon}\,\bar{x}(t)\,\rho_T,$$

where l is the oxide thickness, $\bar{x}(t)$ is the centroid of charge and ρ_T is the total charge in the film. At short times a linear relationship has been found between ΔV_{FB} and $(t)^{1/2}$ (*15, 36, 38, 40*); this was first explained by Snow et al. (*36*) as diffusion in a field-free region and later ascribed to emission from interfacial traps by Hofstein (*15, 38*).

Since the height of the trapping barrier is lowered by the applied field, the rate of the flatband voltage shift is exponentially dependent on the applied field:

$$\Delta V_{FB} \propto (t)^{1/2}\exp\{(-\phi + q\varepsilon\, w/2)/kT\},$$

where ϕ is the trap depth and w is its width. This relationship was first observed in phosphosilicale glass (PSG) layers by Eldridge and Kerr (*41*) and later seen in pure SiO_2 films (*40*). As is apparent from Fig. 6, the behavior is complex and evidence can be seen both for multiple trap levels at low Na concentrations and for a more field-free drift at high levels.

Dielectric Breakdown

Three features of the dielectric strength of SiO_2 films on Si have been studied in detail in the past decade: (1) breakdown of defect free films (*42–46*), (2) statistical uniformity of the dielectric strength (*11*, *18*, *28*), and (3) time dependent breakdown (*17*, *18*, *32*, *40*,

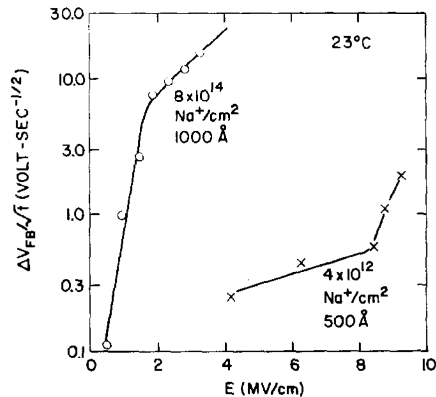

FIG. 6. The rate of flatband voltage shift ($\Delta V_{FB}/(t)^{1/2}$) as a function of applied field for different Na^+ levels. The slope changes probably reflect different Na^+ drift mechanisms (Osburn and Raider (*40*)).

46, 47). The breakdown strength of defect-free films provides information on the basic mechanism involved; it increases slightly with temperature, decreases with substrate doping, and varies with oxide thickness as

$$E_{max} \propto d_{ox}^{-0.21}$$

for films from 100 to 800Å. Prior to breakdown the current becomes unstable (see Fig. 4) and increases with time; positive charge is left in the oxide during this stage. From these observations, it has been concluded that breakdown in SiO_2 films is electronic in nature and involves an impact ionization process; more detailed calculations are currently underway in several laboratories.

Since the dielectric strength of SiO_2 is several times typical FET operating fields, only low-field or defect related breakdown is of primary technological concern. The defect density of the film (as determined from the fraction of low-field breakdown and the capacitor area) varies with a host of processing and material parameters. Wafer cleaning is one key parameter; samples cleaned in a very high temperature ($\approx$ 1300°C) H_2 environment, in which the native oxide is removed, have fewer than 10 breakdown defects/cm^2 (*28*). Cleanliness during the oxidation step is another critical factor; oxidation with a halogen-containing gas addition (C_2HCl_3, CCl_4, Cl_2, HB_r, or HCl) gives markedly better properties; as shown in Fig. 7, the addition of 1–6% HCl can reduce the defect density by a factor of 1/4*x* (*18*); at higher concentrations there is a degradation in the film, presumably because of silicon etching.

Since time dependent breakdown is a FET reliability concern, the subject has been studied and several mechanisms elucidated (*17*, *18*, *32*, *40*, *44*, *46*, *47*). The metal SiO_2 reaction was first identified as a failure mechanism by Chou and Eldridge (*44*) and later seen to occur at relatively low temperatures (100–200°C) where the degradation could take thousands of hours. The time to failure as a result of thermal stress varied nearly as the square of the oxide thickness and depended on the reactivity of the particular electrode material. A second wearout mechanism was related to motion of sodium (*47*, *40*). If the Na concentration was large ($\sim 10^{13}$/cm^2) at least locally, then the space charge field added to the applied field until the breakdown strength was reached and the dielectric failed (*40*). Because of the speed of Na motion, this type of failure usually occurs within one hour of biasing and is very rare for applied fields under 2MV/cm. Wearout has also been observed in films that have no measurable mobile sodium. As seen in Fig. 8, the time to

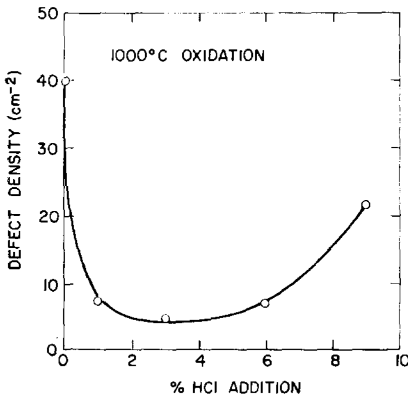

Fig. 7. The effect of HCl additions during Si oxidation on the breakdown defect density of the resulting SiO_2 films.

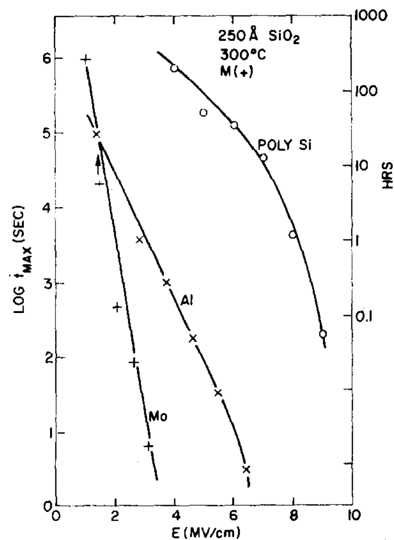

Fig. 8. The maximum time to breakdown, t_{max}, as a function of applied field for SiO_2 films having various electrode materials.

failure depends exponentially on the applied field and is also a strong function of electrode material. Conduction measurements have suggested that breakdown occurs by localized thermal runaway via a localized barrier height lowering. This barrier lowering process has been correlated with the generation of interface states and can be retarded by the introduction of hydrogen into the film either during oxidation (with H_2O, HCl, HBr...), during annealing (in forming gas) or by ion implantation (H_2 or H_2O).

References

1. E. H. Snow, *Solid State Commun.* **5**, 813 (1967).
2. M. Lenzlinger and E. H. Snow, *J. Appl. Phys.* **40**, 278 (1969).
3. C. M. Osburn and E. J. Weitzman, *J. Electrochem. Soc.* **119**, 603 (1972).
4. B. E. Deal, M. Sklar, A. S. Grove and E. H. Snow, *J. Electrochem. Soc.* **114**, 266 (1967).
5. R. J. Kriegler, Y. C. Cheng, and D. R. Colton, *J. Electrochem. Soc.* **119**, 388 (1972).
6. E. H. Nicollian, C. N. Berglund, P. F. Schmidt, and J. M. Andrews, *J. Appl. Phys.* **42**, 5654 (1971).
7. W. Kern and D. A. Puotinen, *RCA Rev.* **31**, 187 (1970).
8. E. Irene, submitted for publication.
9. K. H. Beckmann and N. J. Harrack, *J. Electrochem. Soc.* **118**, 614 (1971).
10. N. Nagasima and H. Enan, *Jap. J. Appl. Phys.* **10**, 441 (1971).
11. R. L. Meek and R. H. Braun, *J. Electrochem. Soc.* **119**, 1538 (1972).
12. T. B. Light, C. M. Osburn, and N. J. Chou, unpublished.
13. G. L. Holmberg, A. B. Kuper, and F. D. Miraldi, *J. Electrochem. Soc.* **117**, 677 (1970).
14. P. F. Schmidt and J. D. Ashner, *J. Electrochem. Soc.* **118**, 325 (1971).
15. S. R. Hofstein, *IEEE Trans. Electron. Devices* **ED14**, 749 (1967).
16. P. Balk, Paper presented at E.C.S. Meeting, Abstract #109, San Francisco, May (1965).
17. C. M. Osburn and N. J. Chou, *J. Electrochem. Soc.* **120**, 1377 (1973).
18. C. M. Osburn, *J. Electrochem. Soc.* **120**, (1974).
19. E. H. Nicollian, A. Goetzberger, and C. N. Berglund, *Appl. Phys. Letters* **15**, 174 (1969).
20. R. S. Powell and C. N. Berglund. *J. Appl. Phys.* **42**, 4390 (1971).
21. E. Yon, W. H. Ko, and A. B. Kuper, *IEEE Trans. Electron. Devices* **ED-13**, 276 (1966).
22. P. H. Robinson and F. P. Heiman, *J. Electrochem. Soc.* **118**, 141 (1971).
23. R. S. Ronen and P. H. Robinson, *J. Electrochem. Soc.* **119**, 747 (1972).
24. R. J. Kriegler, *Appl. Phys. Letters* **20**, 449 (1972).
25. R. J. Kriegler, *Thin Solid Films* **13**, 11 (1972).
26. R. J. Kriegler, "Semiconductor Silicon," p. 363. The Electrochemical Society, New Jersey, 1973.
27. D. R. Young and C. M. Osburn, *J. Electrochem. Soc.* **120**, 1578 (1973).
28. J. M. Green, C. M. Osburn, and T. O. Sedgwick, *J. Electron. Mat.* **3**, 579 (1974).
29. Y. J. van der Meulen, C. M. Osburn, and J. F. Ziegler, *J. Electrochem. Soc.* **120**, 88C (1973).
30. R. L. Meek, *J. Electrochem. Soc.* **120**, 308 (1973).
31. N. J. Chou, C. M. Osburn, Y. J. van der Meulen, and R. Hammer, *Appl. Phys. Letters* **22**, 380 (1973).
32. C. M. Osburn and D. W. Ormond, *J. Electrochem. Soc.* **121**, (1974).
33. T. H. DiStefano, *Appl. Phys. Letters* **19**, 280 (1971).
34. T. H. DiStefano, *J. Appl. Phys.* **44**, 527 (1973).
35. R. Williams and M. H. Woods, *J. Appl. Phys.* **43**, 4142 (1972).
36. E. H. Snow, A. S. Grove, B. E. Deal, and C. T. Sah, *J. Appl. Phys.*, **36**, 1664 (1965).
37. W. A. Pliskin, D. R. Kerr, and J. A. Perri, "Physics of Thin Films," Vol. 4, pp. 257–324, Academic Press, New York, 1967.
38. S. R. Hofstein, *IEEE Trans. Electron. Devices* **ED13**, 222 (1966).
39. D. R. Kerr, *8th Annual Proc. Reliability Phys. Symp.*, p. 1 (1970).
40. C. M. Osburn and S. I. Raider, *J. Electrochem. Soc.* **120**, 1369 (1973).
41. J. M. Eldridge and D. R. Kerr, *J. Electrochem. Soc.* **118**, 986 (1971).
42. N. Klein, *IEEE Trans. Electron. Devices* **ED13**, 788 (1966).
43. C. Fritzsche, *Z. Angew. Phys.* **24**, 43 (1967).
44. N. Chou and J. Eldridge, *J. Electrochem. Soc.* **117**, 1287 (1970).
45. C. M. Osburn and D. W. Ormond, *J. Electrochem. Soc.* **119**, 591, 597 (1972).
46. F. I. Worthing, *J. Electrochem. Soc.* **115**, 88 (1968).
47. S. I. Raider, *Appl. Phys. Letters* **23**, 34 (1973).